

An Efficient Burst Errors Combating for Image Transmission over Mobile WPANs

Mohsen A. M. El-Bendary, Mostafa A. R. El-Tokhy

Abstract—This paper presents an efficient burst error spreading tool. Also, it studies a vital issue in wireless communications, which is the transmission of images over wireless networks. IEEE ZigBee 802.15.4 is a short-range communication standard that could be used for small distance multimedia transmissions. In fact, the ZigBee network is a Wireless Personal Area Network (WPAN), which needs a strong interleaving mechanism for protection against error bursts. Also, it is low power technology and utilized in the Wireless Sensor Networks (WSN) implementation. This paper presents the chaotic interleaving scheme as a data randomization tool for this purpose. This scheme depends on the chaotic Baker map. The mobility effects on the image transmission are studied with different velocity through utilizing the Jakes' model. A comparison study between the proposed chaotic interleaving scheme and the traditional block and convolutional interleaving schemes for image transmission over a correlated fading channel is presented. The simulation results show the superiority of the proposed chaotic interleaving scheme over the traditional schemes.

Keywords—WPANs, Burst Errors, Mobility, Interleaving Techniques, Fading channels.

I. INTRODUCTION

THE utilization of WPANs technologies is became spreading in many fields and applications such as the Wireless Sensor Networks (WSN). The WSN uses in its applications one of WPANs technologies such as Bluetooth, ZigBee, or Ultra Wide Band (UWB). Also, the mobile application of these devices technologies should be considered and the mobility effects on the performance of these networks.

In general, the short-range wireless networks such as Bluetooth and ZigBee are widely used for health care and medical applications [1], [2]. The ZigBee network is a Low-Rate WPAN (LR-WPAN) that is used for short-range, lower complexity of configuration and protocols and low-cost data communication.

Low power consumption in ZigBee networks can be achieved by allowing a device to sleep, which means waking into active mode for brief periods. Enabling such low duty cycle operation is at the heart of the ZigBee standard [3]. ZigBee is built on top of the IEEE 802.15.4 standard. It offers the additional functionality to implement mesh networking rather than point-to-point networking found in most Bluetooth and Wi-Fi applications. The ZigBee specification document is short, allowing a small and simple stack, in contrast to the

other wireless standards such as Bluetooth [4].

TABLE I
IEEE 802.15.4 FREQUENCY BANDS AND DATA RATES

PHY (MHz)	Freq Band (MHz)	Mod.	Channels	Bit Rate (kbps)
868/915	868-868.6	BPSK	1	20
	902-928	BPSK	10	40
2450	2400-2483.5	O-QPSK	16	250

The IEEE 802.15.4 standard is intended to conform to established regulations in Europe, Japan, Canada, and the United States. It defines two physical (PHY) layers; the 2.4 GHz and 868/915 MHz band PHY layers. Although the PHY layer chosen depends on local regulations and user preference, only the higher data rate, worldwide, unlicensed 2.4 GHz Industrial, Scientific and Medical frequency band is considered [5]. A total of 16 channels are available in the 2.4 GHz band, numbered from 11 to 26, each with a bandwidth of 2 MHz, and a channel separation of 5 MHz. The channel mapping frequencies are given in Table I. LR-WPAN output powers are around 0 dBm. LR-WPAN typically operates within a 50-m range. The transmit scheme used is the Direct Sequence Spread Spectrum (DSSS) [6].

The ZigBee network involves little or no infrastructure. It also has a primitive error control mechanism, which is the Automatic Repeat reQuest (ARQ). As a result, this mechanism is unable to reduce the channel effects. So, there is a need for either a coding or interleaving mechanism to combat the bad channel effects [7].

Several papers have studied the transmission of images with the IEEE 802.15.4 standard. In [8], the authors studied the process of image fragmentation for transmission over the ZigBee network. In the case of transmission over mobile networks, there is a probability of burst errors. The burst errors have a bad effect on the transmitted data and image. In this paper, we try to decrease the effect of error bursts on the transmission of images by introducing a powerful chaotic interleaver.

The paper is organized as follows. In Section II, ZigBee packet format is introduced. In Section III, the proposed modifications are presented. In Section IV, the simulation assumptions and the simulation results are presented. Finally, the conclusion is presented in Section V.

Mohsen A. M. El-Bendary is with the Helwan University, Cairo, Egypt (phone: 002-0128-8712859; e-mail: mohsenbendary@hotmail.com, engmohsen2004@yahoo.com).

Mostafa A. El-Tokhy is with the Helwan University, Cairo, Egypt (e-mail: mostafaeltokhy2717@yahoo.com).

II. ZIGBEE PACKET FORMAT

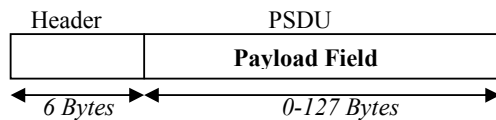


Fig. 1 ZigBee packet format

The structure of the ZigBee packet is shown in Fig. 1. The header contains three fields; a preamble of 32 bits for synchronization, a packet delimiter of 8 bits, and a physical header of 8 bits. The Physical Service Data Unit (PSDU) field contains a payload of 0 to 127 bytes length. The ZigBee network uses an error detection/retransmission technique. To ensure successful reception of data, an acknowledged frame delivery protocol is supported to increase transfer reliability [9]. The ZigBee network uses the DSSS technique for data transmission, because it increases the immunity to interference. It is based on the multiplication of the original binary stream with a wideband Pseudo Noise (PN) spreading code, which results in a wideband continuous time scrambled signal. DSSS significantly improves protection against interfering signals, especially narrowband signals. It also provides a multiple access capability, when the several different spreading codes are being used, simultaneously. It also provides a transmission security. DSSS is also used as a technique to generate Ultra Wide Band (UWB) signals [9]. As shown in Fig. 2, the output signal of the modulator $m(t)$ has a much larger bandwidth than the input signal $d(t)$ [10]-[12].

Fig. 2 shows the stages of the DSSS technique. At the receiver, the wideband signal is despread as shown in Fig. 2. The chip rate C is much larger than the input data rate R .

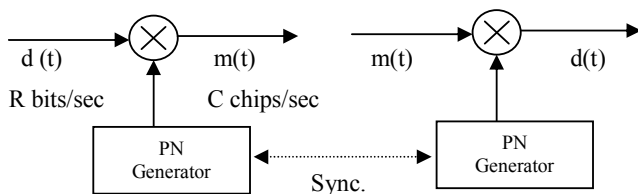


Fig. 2 The direct sequence spread spectrum technique

III. PROPOSED MODIFICATIONS

The transmission of multimedia over unreliable data links has become a topic of paramount importance. This type of transmission must reconcile the high data rates involved in multimedia contents and the noisy nature of the channels, be it wireless or mobile. In this paper, we try to improve the transmission of images over the ZigBee network with different interleaving schemes. We study the feasibility of data interleaving prior to transmission over ZigBee networks. The paper presents a new chaotic interleaver and compares it to the traditional block and convolutional interleavers.

A. Block Interleaver Scheme

The block interleaving can be used for image transmission with the ZigBee network. After converting the image into a binary sequence, this sequence is rearranged into a matrix in a

row-by-row manner, and then read from the matrix in a column-by-column manner. Now take a look at how the block interleaving mechanism can correct error bursts. Assume an error burst affecting four consecutive bits (1-D error burst) as shown in Fig. 3 (b) with shades. After de-interleaving as shown in Fig. 3 (c), the error burst is effectively spread among four different rows, resulting in a small effect for the 1-D error burst. With a single-error correction capability, it is obvious that no decoding error will result from the presence of such 1-D error burst. This simple example demonstrates the effectiveness of the block interleaving mechanism in combating 1-D error bursts. Let us examine the performance of the block interleaving mechanism, when a 2-D (2×2) error burst occurs [13], as shown in Fig. 3 (b) with shades. Fig. 3 (c) indicates that this 2×2 error burst has not been spread, effectively, so that there are adjacent bits in error in the first and second rows. As a result, this error burst cannot be corrected using a single-error correction mechanism. That is, the block interleaving mechanism cannot combat the 2×2 error bursts.

B. Convolutional Interleaver Scheme

The convolutional interleaver is constructed by T parallel branches. Each line contains a shift register with a predefined length [14]. The input data is fed into the branches of the interleaver and the output data is taken from the outputs of these branches. In the computer simulations, the length of the interleaver input is 1024 bits, which is the length of the whole payload in ZigBee packets [15].

C. Chaotic Interleaver Scheme

As mentioned in the previous section, the block interleaver is not efficient with 2-D error bursts. As a result, there is a need for an advanced interleaver for this task. The 2-D chaotic Baker map in its discretized version is a good candidate for this purpose. After rearrangement of bits into a 2-D format, the chaotic Baker map is used to randomize the bits. The discretized Baker map is an efficient tool to randomize the items in a square matrix. Let $B(n_1, \dots, n_k)$, denote the discretized map, where the vector, $[n_1, \dots, n_k]$, represents the secret key, S_{key} . Defining N as the number of data items in one row, the secret key is chosen such that each integer n_i divides N , and $n_1 + \dots + n_k = N$ [16]-[20].

$$B(r, s) = \left[\frac{N}{n_1} (r - N) + s \bmod \left(\frac{N}{n_1} \right), \frac{n_i}{N} \left(s - s \bmod \left(\frac{N}{n_i} \right) + N_i \right) \right] \quad (1)$$

where $N_i \leq r < N_i + n_i, 0 \leq s < N$, and $N_1 = 0$.

With using this formula and its variable, the chaotic permutation is performed as follows steps:

- 1- An $N \times N$ square matrix is divided into N rectangles of width n_i and number of elements N .
- 2- The elements in each rectangle are rearranged to a row in the permuted rectangle. Rectangles are taken from right to left beginning with upper rectangles then lower ones.

- 3- Inside each rectangle, the scan begins from the bottom left corner towards upper elements.

Fig. 4 shows an example for chaotic interleaving of an 8×8 square matrix (i.e. $N = 8$). The secret key, $\text{Skey} = [n_1, n_2, n_3] = [2, 4, 2]$. Note that, the chaotic interleaving mechanism has a better treatment to both 1-D and 2-D error bursts than the block interleaving mechanism. Errors are better distributed to

bits after de-interleaving in the proposed chaotic interleaving scheme. As a result, a better Peak Signal to Noise Ratio (PSNR) of received images can be achieved with this proposed mechanism. Moreover, it adds a degree of security to the communication system. At the receiver of the ZigBee system, a chaotic de-interleaving step is performed.

b_1	b_2	b_3	b_4	b_5	b_6	b_7	b_8	b_1	b_9	b_{17}	b_{25}	b_{33}	b_{41}	b_{49}	b_{57}	b_1	b_2	b_3	b_4	b_5	b_6	b_7	b_8
b_9	b_{10}	b_{11}	b_{12}	b_{13}	b_{14}	b_{15}	b_{16}	b_2	b_{10}	b_{18}	b_{26}	b_{34}	b_{42}	b_{50}	b_{58}	b_9	b_{10}	b_{11}	b_{12}	b_{13}	b_{14}	b_{15}	b_{16}
b_{17}	b_{18}	b_{19}	b_{20}	b_{21}	b_{22}	b_{23}	b_{24}	b_3	b_{11}	b_{19}	b_{27}	b_{35}	b_{43}	b_{51}	b_{59}	b_{17}	b_{18}	b_{19}	b_{20}	b_{21}	b_{22}	b_{23}	b_{24}
b_{25}	b_{26}	b_{27}	b_{28}	b_{29}	b_{30}	b_{31}	b_{32}	b_4	b_{12}	b_{20}	b_{28}	b_{36}	b_{44}	b_{52}	b_{60}	b_{25}	b_{26}	b_{27}	b_{28}	b_{29}	b_{30}	b_{31}	b_{32}
b_{33}	b_{34}	b_{35}	b_{36}	b_{37}	b_{38}	b_{39}	b_{40}	b_5	b_{13}	b_{21}	b_{29}	b_{37}	b_{45}	b_{53}	b_{61}	b_{33}	b_{34}	b_{35}	b_{36}	b_{37}	b_{38}	b_{39}	b_{40}
b_{41}	b_{42}	b_{43}	b_{44}	b_{45}	b_{46}	b_{47}	b_{48}	b_6	b_{14}	b_{22}	b_{30}	b_{38}	b_{46}	b_{54}	b_{62}	b_{41}	b_{42}	b_{43}	b_{44}	b_{45}	b_{46}	b_{47}	b_{48}
b_{49}	b_{50}	b_{51}	b_{52}	b_{53}	b_{54}	b_{55}	b_{56}	b_7	b_{15}	b_{23}	b_{31}	b_{39}	b_{47}	b_{55}	b_{63}	b_{49}	b_{50}	b_{51}	b_{52}	b_{53}	b_{54}	b_{55}	b_{56}
b_{57}	b_{58}	b_{59}	b_{60}	b_{61}	b_{62}	b_{63}	b_{64}	b_8	b_{16}	b_{24}	b_{32}	b_{40}	b_{48}	b_{56}	b_{64}	b_{57}	b_{58}	b_{59}	b_{60}	b_{61}	b_{62}	b_{63}	b_{64}

(a)

(b)

(c)

Fig. 3 Block interleaving of an 8×8 matrix (a) The 8×8 matrix. (b) Block interleaving of the matrix. (c) Effect of error bursts after de-interleaving

b_1	b_2	b_3	b_4	b_5	b_6	b_7	b_8	b_{31}	b_{23}	b_{15}	b_7	b_{32}	b_{24}	b_{16}	b_8	b_1	b_2	b_3	b_4	b_5	b_6	b_7	b_8
b_9	b_{10}	b_{11}	b_{12}	b_{13}	b_{14}	b_{15}	b_{16}	b_{63}	b_{55}	b_{47}	b_{39}	b_{64}	b_{56}	b_{48}	b_{40}	b_9	b_{10}	b_{11}	b_{12}	b_{13}	b_{14}	b_{15}	b_{16}
b_{17}	b_{18}	b_{19}	b_{20}	b_{21}	b_{22}	b_{23}	b_{24}	b_{11}	b_3	b_{12}	b_4	b_{13}	b_5	b_{14}	b_6	b_{17}	b_{18}	b_{19}	b_{20}	b_{21}	b_{22}	b_{23}	b_{24}
b_{25}	b_{26}	b_{27}	b_{28}	b_{29}	b_{30}	b_{31}	b_{32}	b_{27}	b_{19}	b_{28}	b_{20}	b_{29}	b_{21}	b_{30}	b_{20}	b_{25}	b_{26}	b_{27}	b_{28}	b_{29}	b_{30}	b_{31}	b_{32}
b_{33}	b_{34}	b_{35}	b_{36}	b_{37}	b_{38}	b_{39}	b_{40}	b_{43}	b_{35}	b_{44}	b_{36}	b_{45}	b_{37}	b_{46}	b_{38}	b_{33}	b_{34}	b_{35}	b_{36}	b_{37}	b_{38}	b_{39}	b_{40}
b_{41}	b_{42}	b_{43}	b_{44}	b_{45}	b_{46}	b_{47}	b_{48}	b_{59}	b_{51}	b_{60}	b_{52}	b_{61}	b_{53}	b_{62}	b_{54}	b_{41}	b_{42}	b_{43}	b_{44}	b_{45}	b_{46}	b_{47}	b_{48}
b_{49}	b_{50}	b_{51}	b_{52}	b_{53}	b_{54}	b_{55}	b_{56}	b_{25}	b_{17}	b_9	b_1	b_{20}	b_{18}	b_{10}	b_2	b_{49}	b_{50}	b_{51}	b_{52}	b_{53}	b_{54}	b_{55}	b_{56}
b_{57}	b_{58}	b_{59}	b_{60}	b_{61}	b_{62}	b_{63}	b_{64}	b_{57}	b_{49}	b_{41}	b_{33}	b_{58}	b_{50}	b_{42}	b_{34}	b_{57}	b_{58}	b_{59}	b_{60}	b_{61}	b_{62}	b_{63}	b_{64}

(a)

(b)

(c)

Fig. 4 Chaotic interleaving of an 8×8 matrix (a) The 8×8 matrix divided into rectangles (Shaded bits are bits affected by error bursts). (b) Chaotic interleaving of the matrix. (c) Effect of error bursts after de-interleaving.

IV. SIMULATION RESULTS

In this section, the computer simulation results are presented. An important assumption used in the simulation is that a packet is discarded if there is an error in either the header or the payload field [21]. This is a realistic assumption to simulate the real ZigBee system operation. A correlated Rayleigh fading channel is used. The channel model utilized is the Jake's model [22], [23]. The assumed mobile ZigBee device velocity is 10 miles/hour, and the carrier frequency is 2.46 GHz. The Doppler spread is 36.6 Hz. Fig. 5 gives the original Cameraman image used in the experiments. It is the Matlab image and its format is Tag Image File format (TIF).

The image binary sequence to be transmitted is fragmented into packets. The PSNR of the received images is used as an evaluation metric in this paper.

The computer simulation section contains four categories of experimental simulations. The first section studied the mobility effects on the image transmission with different

velocity. In the simulation experiments, the interference is neglected and simulation results proposed the path loss is ignored with the short range of the ZigBee network.



Fig. 5 Original Cameraman image

This section of experiments is devoted for studying the

effects of the mobility of the ZigBee device (V_c) on the transmitted packets and the received images. The ZigBee employs the 16-bit Cyclic Redundancy Check (CRC) for error detecting scheme. In this computer experiment, the V_c is 1, 10, 20, 30, and 40 miles/hour. Figs. 6 and 7 give the received images at SNR= 10 and 20 dB, respectively. Fig. 8 shows the PSNR variation of the received images with the channel SNR.

As shown in the previous experiments, the mobility has bad effects on the PSNR values of the received images. These experiments studied different velocity of the mobile terminal with different SNR of the communication channels.

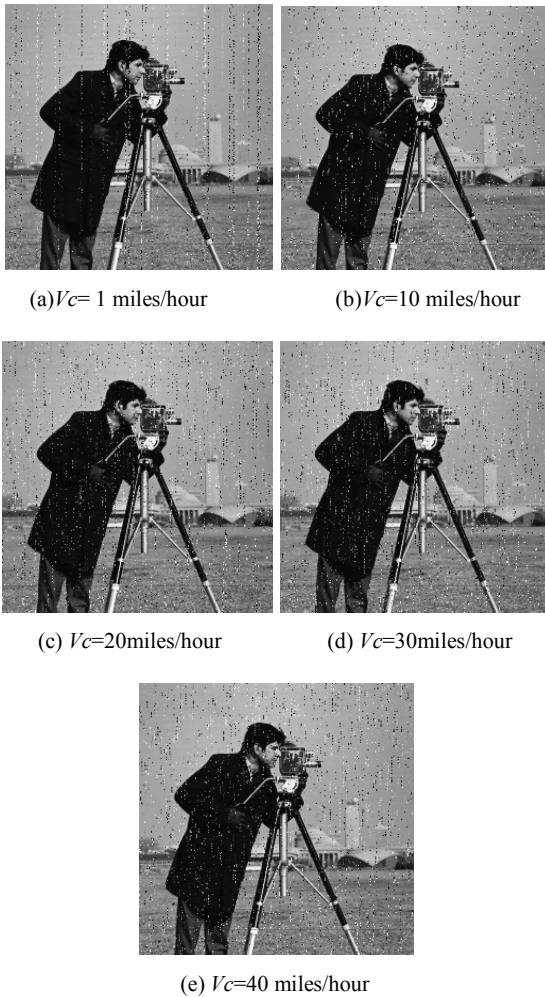


Fig. 6 Received Cameraman image over a correlated fading channel at SNR =10 dB with (a) PSNR=22.7 dB, (b) PSNR=21.7 dB, (c) PSNR=21.6 dB, (d) PSNR=21.5dB, and (e) PSNR=21.3dB

Fig. 6 gives the results of the received image samples with the channel SNR =10 dB, with the velocity variation 1, 10, 20, 30 and 40 mile per hour the PSNR of the received image samples 22.7, 21.7, 21.6, 21.5, and 21.3 dB respectively. As shown in the results, the PSNR is taken as image quality metric, lower PSNR value means low received image quality.

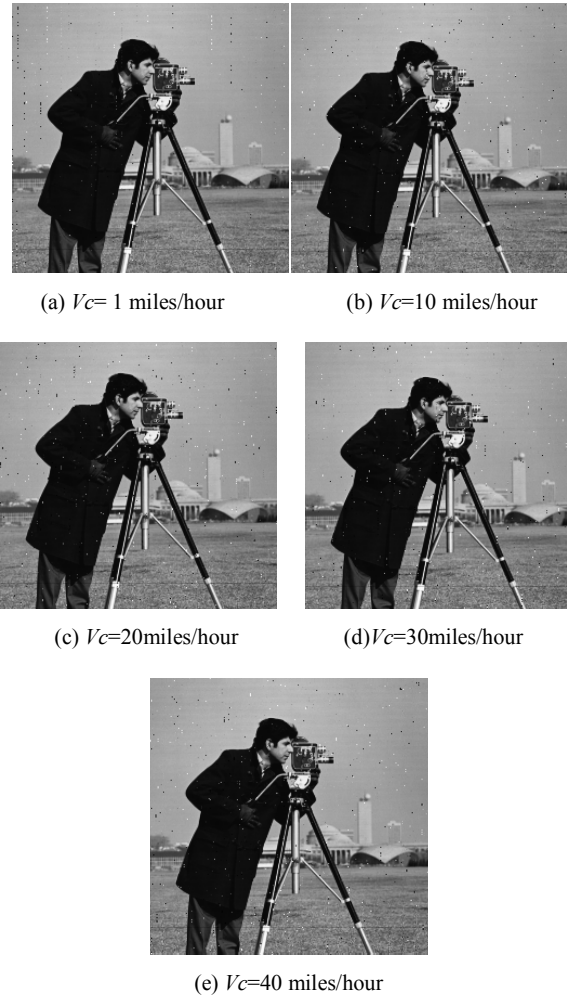


Fig. 7 Received Cameraman image over a correlated fading channel at SNR =20 dB with (a) PSNR=33.47 dB, (b) PSNR=31.97 dB, (c) PSNR=31.38 dB, (d) PSNR=31.07 dB, and (e) PSNR=31.0 dB

Fig. 7 gives the results of the received image samples with the channel SNR =20 dB, with the velocity variation 1, 10, 20, 30 and 40 mile per hour the PSNR of the received image samples 33.47, 31.97, 31.38, 31.07, and 31.0 dB respectively. As shown in the results, the PSNR of the received image samples is enhanced with channel SNR increasing. Also, the result reveals that the variation between the PSNR of the image samples is increased.

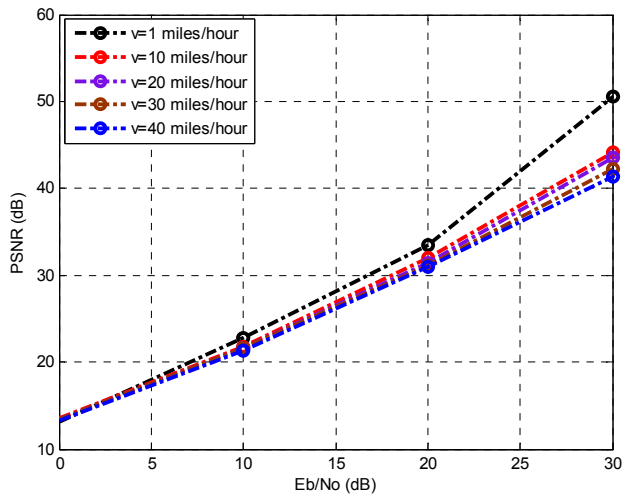


Fig. 8 PSNR vs. SNR for the received Cameraman image over the ZigBee standard with the different V_c .

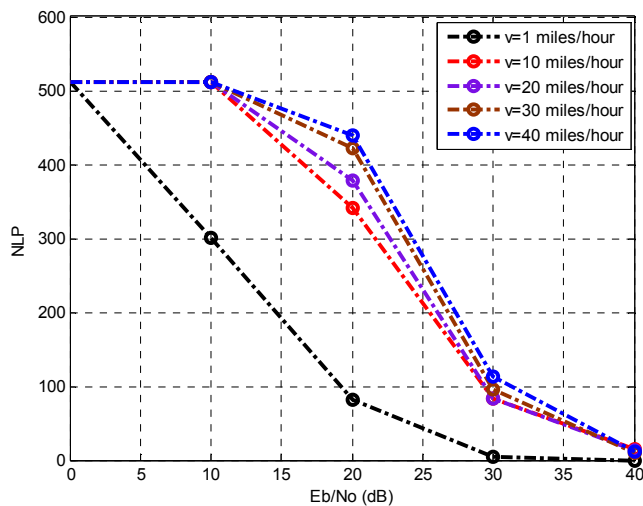


Fig. 9 NLP vs. SNR for the received Cameraman image over the ZigBee standard with the different V_c .

This section of experiments evaluates the effect of mobility on the image transmission over the ZigBee network. There are many metric are used for this purpose. As shown in the previous Figs. 7-9, the received image samples with different velocity and different SNR of channel and the PSNR of the received images are used.

Also, the number of Lost Packets (NLP) is used as a metric for measuring the mobility effects. Fig. 9 gives the NLP variation with the channel SNR. It is clear that with increasing the V_c of the terminal, the NLP is increased.

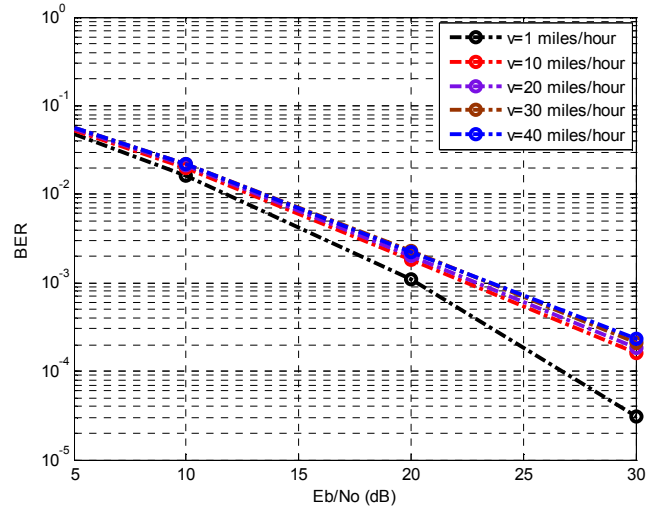


Fig. 10 BER vs. SNR for the received Cameraman image over the ZigBee standard with the different V_c .

The mobility effects on the error performance of the ZigBee network through BER variation with the channel SNR is shown in Fig. 10. It is clear that with increasing the V_c of the terminal, the error performance of the system is degraded.

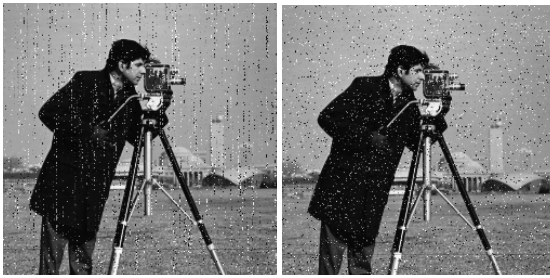
In the following, the different interleaving mechanisms are presented. There are different scenarios are employed for the image transmission over the ZigBee network. In the first computer simulation, the Cameraman image is transmitted over a correlated fading channel with Signal to Noise Ratio (SNR) = 10 dB. Three scenarios of no interleaving, block interleaving, convolutional interleaving and chaotic interleaving are considered for comparison. The results of this experiment are shown in Fig. 11. From these results, it is clear that the effect of all interleaving schemes is approximately equal at low SNR values.

The computer based experiments are devoted to investigate the performance of different proposed scenarios with the same velocity value for every experiment with variety channel SNR. As shown in Fig. 12, the interleaving techniques, no-interleaving, traditional block interleaving, convolutional interleaving and the proposed chaotic interleaving are utilized; with the same V_c , the PSNR of the image samples is 31.1, 31.5, 32.1, and 33.2 dB, respectively, with the SNR of channel is 20 dB.



(a) No interleaving

(b) Block interleaving



(c) Convolutional interleaving (d) Chaotic Interleaving

Fig. 11 Received Cameraman image over a correlated fading channel at SNR =10 dB with (a) PSNR=21.3 dB, (b) PSNR=21.4 dB, (c) PSNR=21.1 dB, and (d) PSNR=21.5 dB



(a) No interleaving (b) Block interleaving



(c) Convolutional interleaving (d) Chaotic interleaving

Fig. 12 Received Cameraman image over a correlated fading channel at SNR=20 dB with (a) PSNR=31.1 dB, (b) PSNR=31.5dB, (c) PSNR=32.1 dB, and (d) PSNR=33.2 dB



(a) No interleaving (b) Block interleaving



(c) Convolutional interleaving (d) Chaotic interleaving.

Fig. 13 Received Cameraman image over a correlated fading channel at SNR=30 dB with (a) PSNR=39.1 dB, (b) PSNR=41 dB, (c) PSNR=41.1 dB, and (d) PSNR=43.1 dB

Other experiments are repeated with SNR = 20 and 30 dB and the results are shown in Figs. 12, 13, respectively. From these results, we notice that the chaotic interleaver outperforms the other interleavers at moderate to high SNRs.

For the comparison purpose, the variation of the PSNR of the received image, the number of lost frames and the Bit Error Rate (BER) with the channel SNR are studied and the results are shown in Figs. 14-16. From these results, it is clear the chaotic interleaver enhancement begins at medium SNR values.

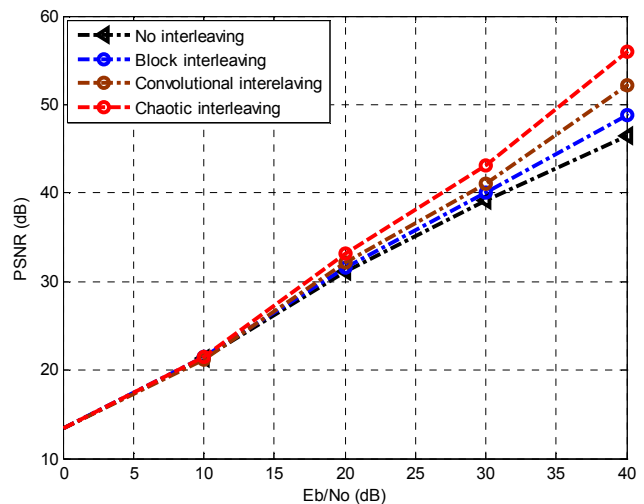


Fig. 14 PSNR vs. SNR for the received Cameraman image over a correlated fading channel

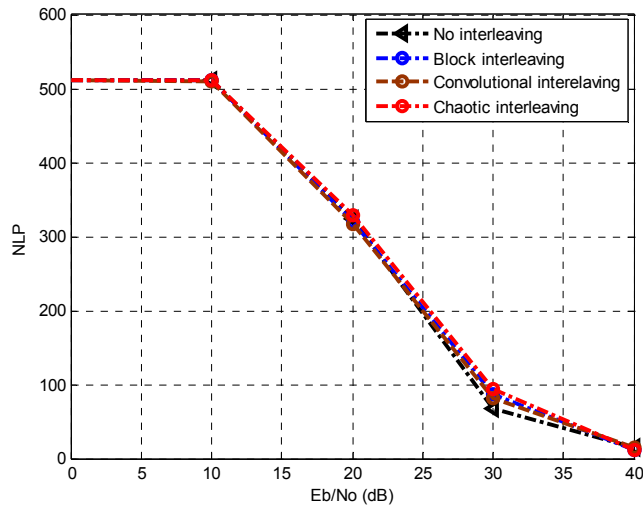


Fig. 15 Number of lost frames vs. SNR for the received Cameraman image over a correlated fading channel

As shown in this Figs. 14, 15, the proposed chaotic interleaver does not decrease the number of lost frames, but it enhances the PSNR of the received images at medium to high SNR values. The powerful of the proposed technique due to the ZigBee standard doesn't employ error control codes scheme with the transmitted packets. So, there is the possibility using of the chaotic interleaver over the mobile ZigBee network for improve the received image quality with the security enhancing.

As shown in the results of the previous experiments computer simulation based, the proposed chaotic interleaver does not decrease the number of lost frames, but it enhances the PSNR of the received images at medium to high SNR values. The powerful of the proposed technique due to the ZigBee standard doesn't employ error control codes scheme with the transmitted packets. So, there is the possibility using of the chaotic interleaver over the mobile ZigBee network for improve the received image quality with the security enhancing.

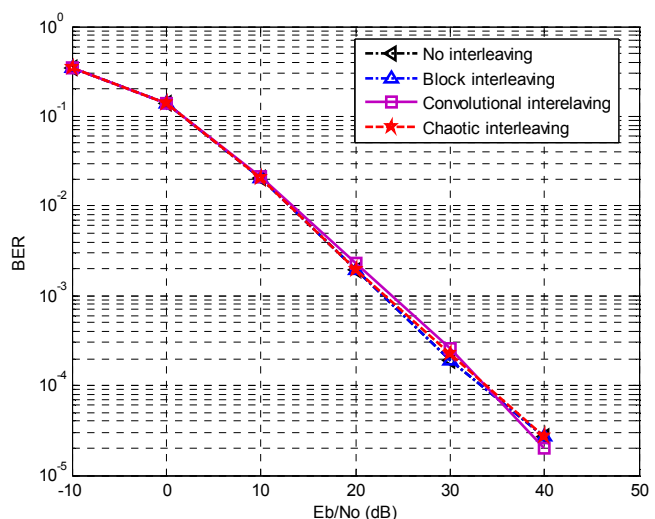


Fig. 16 BER vs. SNR for the received Cameraman image over a correlated fading channel

As shown in the NPL and BER metrics, the results of the experiments scenarios are much closed. These results can be briefed in the following, that the interleaving technique spread the errors and decreases the burst error effects but it does not reduce the number of errors. So, the number of lost packets in the scenarios is much closed. The simulation experiments revealed that the presented proposed method of interleaving enhanced the received images with increasing the running time. To decreasing this time, the process of the proposed approach is applied on bit-by-bit of the digital images.

V. CONCLUSION

This paper presented a simple and efficient data randomization tool using the chaotic interleaver for combating the burst errors effect on the transmission of images over the mobile WPANs. Also, it presents the mobility effects on the image transmission with different velocity. A comparison study between the proposed interleaver and the conventional interleavers has been presented. The computer simulation results have revealed the effectiveness of the proposed interleaver tool at medium and high SNR values. Also, the proposed technique enhanced the security level over the ZigBee network link with using the secret key which is used for randomizing the data, as it is based on chaotic map encryption. The secret key can be changed every transmitted packet for providing secured and trusted wireless link.

REFERENCES

- [1] ZigBee Alliance, available at <http://www.zigbee.org/>, 2009.
- [2] The Wi-Fi Alliance, available at <http://www.wi-fi.org/>, 2009.
- [3] B. Kai, and P. Yong, "Performance Study on ZigBee-Based Wireless Personal Area Networks for Real-Time Health monitoring", ETRI Journal, Volume 28, No. 4, Aug. 2006.
- [4] Jin-Shyan Lee, Yu-Wei Su, and Chung-Chou Shen, "A Comparative Study of Wireless Protocols: Bluetooth, UWB, ZigBee, and Wi-Fi", The 33rd Annual Conference of the IEEE Industrial Electronics Society (IECON), Nov. 5-8, 2007, Taipei, Taiwan.

- [5] W. Guo and M. Zhou, "An emerging technology for improved building automation control", IEEE International Conference on Systems, man and Cybernetics, 2009. SMC 2009., pp.337-342, Oct. 2009.
- [6] B. Sidhu, H. Singh, and A. Chhabra, "Emerging Wireless Standards - WiFi, ZigBee and WiMAX s", World Academy of Science, Engineering and Technology 25 2007.
- [7] S. Vafi, and T. Wysocki, "Performance of convolutional interleavers with different spacing parameters in turbo codes," Proc. 6th Australian Workshop on Communications Theory, 2005, pp. 8-12.
- [8] G. Pechterev, Z. Sahinoglu, P. Orlik, and G. Bhatti, "Image Transmission over IEEE 802.15.4 and ZigBee Networks," IEEE ISCAS May 2005, Kobe Japan.
- [9] L. Ozarow, S. Shamai, and A.D. Wyner, "Information theoretic considerations for cellular mobile radio," IEEE Trans. Veh. Tech., vol. 43, pp. 359-378, 1994.
- [10] Emad N. Farag, Mohamed I Elmasry, Mixed Signal VLSI Wireless Design Circuits and System, 1st Edition, Kluwer Academic Publishers, 1999.
- [11] H. S. Kim and H. K. Lee, "Modified Beacon-Enabled IEEE-802.15.4 MAC for lower latency", Mitsubishi Electric Research laboratories, 2009, 201 Broadway, Cambridge, Massachusetts 02139.
- [12] T. S. Rappaport, "Wireless Communications", Prentice Hall 1996.
- [13] S. H. Lee and E. K. Joo, "The Effect of Block Interleaving in an LDPC-Turbo Concatenated Code", ETRI Journal, Volume 28, Number 5, October 2006
- [14] S. Vafi, T. A. Wysocki, "Application of convolutional interleavers in turbo codes with unequal error protection", JTIT, Journal of Telecommunication and Information technology, Jan. 2006.
- [15] G. Pechterev, Z. Sahinoglu, P. Orlik, and G. Bhatti, "Error Protection for Progressive Image Transmission Over Memoryless and Fading Channels", IEEE Transactions on Communications, Vol. 46, No. 12, Dec. 1998.
- [16] A. N. Lemma, J. Aprea, W. Oomen, and L. V. de Kerkhof, "A Temporal Domain Audio Watermarking Technique", IEEE Transactions on Signal Processing, Vol. 51, No. 4, pp. 1088-1097, 2003.
- [17] W. Li, X. Xue, and P. Lu, "Localized Audio Watermarking Technique Robust Against Time-Scale Modification", IEEE Transactions on Multimedia, Vol. 8, No. 1, pp. 60-69, 2006.
- [18] G. Voyatzis and I. Pitas, "Chaotic Watermarks for Embedding in the Spatial Digital Image Domain," Proc. IEEE Int. Conference Image Processing, Vol. 2, pp. 432-436, Oct. 1998.
- [19] R. Liu and T. Tan, "An SVD-Based Watermarking Scheme for Protecting Rightful Ownership", IEEE Transactions On Multimedia, Vol. 4, No. 1, pp. 121-128, MARCH 2002.
- [20] Z. Liu and A. Inoue, "Audio Watermarking Techniques Using Sinusoidal Patterns Based on Pseudorandom Sequences", IEEE Transactions On Circuits And Systems For Video Technology, Vol. 13, No. 8, pp. 801-812, 2003.
- [21] M. A. M. Mohamed, A. Abou El-Azm, N. El-Fishwy, M. A. R. El-Tokhy, F. E. Abd El-Samie, "Optimization of Bluetooth Packet Format for Efficient Performance," Progress in Electromagnetic Research M, Vol. 1, 101-110, 2008.
- [22] W. C. Jakes, "Microwave Mobile Communications," New York, John Wiley & Sons Inc. ISBN 0-471-43720-4, 1-Feb. 1975.
- [23] Aldrich, "Correlations Genuine and Spurious in Pearson and Yule," Statistical Science 10: 364-376. <http://www.jstor.org/stable/2246135>.



Mohsen A. M. Mohamed Kaseem El-Bendary received his BS in 1998, MSc in 2008, PhD in 2012 all in communication engineering, from Menoufia University, Faculty of electronic Engineering. He is now a lecturer in Electronics dept., Helwan University, Cairo, Egypt. His research interests cover wireless networks, wireless technology, channel coding, QoS over Bluetooth system and Wireless Sensor Network (WSN), and security systems which use wireless technology, such as fire alarm and

access control systems.